JACS
JOURNAL OF THE AMERICAN CHEMICAL SOCIETY
Communication
pubs.acs.org/JACS

Proposed Ligand-Centered Electrocatalytic Hydrogen Evolution and Hydrogen Oxidation at a Noninnocent Mononuclear Metal−Thiolate

Andrew Z. Haddad, Davinder Kumar, Kagna Ouch Sampson, Anna M. Matzner, Mark S. Mashuta, and Craig A. Grapperhaus*

Department of Chemistry, University of Louisville, 2320 South Brook Street, Louisville, Kentucky 40292, United States

Supporting Information

ABSTRACT: The noninnocent coordinatively saturated mononuclear metal−thiolate complex ReL_3 (L = diphenylphosphinobenzenethiolate) serves as an electrocatalyst for hydrogen evolution or hydrogen oxidation dependent on the presence of acid or base and the applied potential. ReL_3 reduces acids to H_2 in dichloromethane with an overpotential of 380 mV and a turnover frequency of 32 ± 3 s^{-1}. The rate law displays a second-order dependence on acid concentration and a first-order dependence on catalyst concentration with an overall third-order rate constant (k) of 184 ± 2 M^{-2} s^{-1}. Reactions with deuterated acid display a kinetic isotope effect of 9 ± 1. In the presence of base, ReL_3 oxidizes H_2 with a turnover frequency of 4 ± 1 s^{-1}. The X-ray crystal structure of the monoprotonated species $[Re(LH)L_2]^+$, an intermediate in both catalytic H_2 evolution and oxidation, has been determined. A ligand-centered mechanism, which does not require metal hydride intermediates, is suggested based on similarities to the redox-regulated, ligand-centered binding of ethylene to ReL_3.

The potential use of hydrogen gas as a clean energy carrier has initiated substantial interest in the development of catalysts for hydrogen evolving reactions (HERs).[1] The energy stored within the H_2 molecule can be recovered in a fuel cell through the catalyzed oxidation of H_2 to protons, which is the reverse of a HER. This strategy of energy storage/recovery occurs in nature with the assistance of hydrogenase enzymes with H_2 evolution and H_2 oxidation generally favored by [FeFe]- and [NiFe]-hydrogenases, respectively.[2−5] A renaissance in the development of small molecule catalysts for HERs was sparked by Dubois and Bullock's nickel catalysts including $[Ni(P^{Me}{}_2N^{Ph}{}_2)_2](BF_4)_2$ ($P^{Me}{}_2N^{Ph}{}_2$ = 1,5-diphenyl-3,7-dimethyl-1,5-diaza-3,7-diphosphacyclooctane), which incorporates a proximal base to reduce protons with a high turnover frequency (TOF = 6700 s^{-1}) and a low overpotential (545 mV).[6−9] Subsequently, numerous H_2 evolution catalysts were reported including a number of metal-dithiolene complexes with high TOF.[10−15] Despite these advances, few H_2 oxidation catalysts are known and even fewer complexes catalyze the reaction in both directions.[16,17] In this Communication, we report electrocatalytic H_2 evolution and H_2 oxidation using the noninnocent mononuclear metal−thiolate complex ReL_3 (L = diphenylphosphinobenzenethiolate). ReL_3 catalytically oxidizes H_2 in the presence of base at potentials greater than 0.42 V, as well as catalytically evolving H_2 from acid at potentials less than −1.60 V, Scheme 1.

Scheme 1. Electrocatalysis with ReL_3

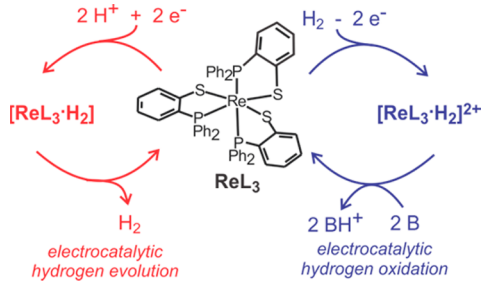

Our approach employs a coordinatively saturated metal complex with a known redox-active ligand core.[18,19] The electrocatalyst ReL_3 displays a reversible $Re^{III/II}$ reduction at −1.60 V and two reversible, noninnocent oxidations at −0.34 and +0.42 V (versus ferrocenium/ferrocene).[19] The noninnocence of the ligands is attributed to covalent metal−sulfur interactions that result in frontier molecular orbitals with significant metal-d and sulfur-p character as also observed for ReL_3 and RuL_3.[19,20] As a result, while $[ReL_3]^+$ contains a *formal* Re^{IV}, the complex has some Re^{III}-thiyl radical character and the *formal* Re^{V} of $[ReL_3]^{2+}$ has Re^{IV}-thiyl and Re^{III}-dithiyl radical character. Further, the symmetry of the frontier molecular orbitals inhibits disulfide bond formation, but favors ethylene addition.[19−21] Accordingly, oxidation of ReL_3 in the presence of ethylene results in ligand-centered ethylene addition generating Re-dithioethers $[ReL_3{\cdot}C_2H_4]^n$ (n = 0, 1, 2). Notably, ethylene binding affinities span 20 orders of magnitude as a function of the complex charge, n.[18,19] Given their similarities in the frontier molecular orbitals, we reasoned that H_2 may display similar reactivity with ReL_3 as ethylene (see Supporting Information).

Upon addition of acetic acid to CH_2Cl_2 solutions of ReL_3 the cathodic current at −1.70 V increases indicative of electrocatalytic reduction (Figure 1A). At acid concentrations above 0.4 M, the current is acid-independent indicating the catalyst is acid saturated.[22−25] Under these pseudo-first order conditions, the turnover frequency (TOF), which is also the observed rate constant, is 30 ± 4 s^{-1}. Hydrogen evolution using sulfuric acid as the H^+ source yields a statistically equivalent TOF of 32 ± 3 s^{-1}.

Received: May 29, 2015
Published: July 10, 2015

DOI: 10.1021/jacs.5b05561
J. Am. Chem. Soc. 2015, 137, 9238−9241

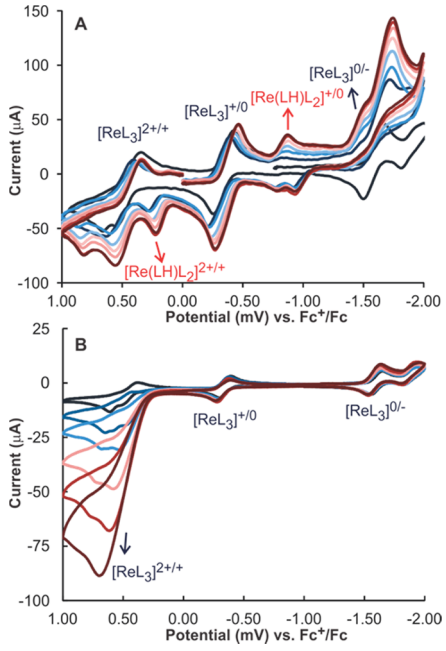

Figure 1. Cyclic voltammograms of 0.3 mM ReL_3 in CH_2Cl_2 (0.1 M Bu_4NPF_6) at a glassy carbon electrode showing (A) H_2 evolution upon successive addition of acetic acid (0.30 M max.) and (B) H_2 oxidation upon successive addition of Et_3N (0.80 mM max).

The overpotential for hydrogen evolution is 380 mV with either acid source. Control experiments with acetic acid in the absence of $[ReL_3]$ show no significant current in the potential window.

In addition to electrocatalytic hydrogen evolution, ReL_3 also catalyzes H_2 oxidation. Addition of triethylamine to ReL_3 under 1 atm of H_2 (Figure 1B) increases anodic current near the formal $Re^{V/IV}$ couple. At concentrations above 0.8 mM, the catalytic current is base-independent and a TOF of 4 ± 1 s^{-1} was determined at an overpotential of 670 mV.[26,27] Control experiments with triethylamine/H_2, but no ReL_3, show no significant current.

The robustness of the catalyst was demonstrated in controlled potential bulk electrolysis experiments. At an applied potential of −1.8 V vs ferrocenium/ferrocene, ReL_3 catalytically evolved H_2 from CH_2Cl_2 containing 0.05 M acetic acid with turnover numbers (TON) of 13.6 and 54.0 after 1.5 and 6 h, respectively. Under these conditions, the TOF remains at ∼9 h^{-1} with no significant decrease in HER activity over 6 h. The gas evolved during electrolysis was confirmed as H_2 by gas chromatography analysis of headspace. After 6 h, the headspace consisted of 22% H_2 indicating a *minimum* Faradaic efficiency of 73%, although the actual value may be higher as some H_2 escaped during electrolysis.

The complex ReL_3 catalyzes H_2 evolution approximately 8 times faster than it catalyzes H_2 oxidation. The TOF for H_2 evolution is statistically equivalent for weak and strong acids, suggesting the two share a common rate-determining step. The rate-determining step is assigned as H_2 release based on a second-order acid dependence under nonsaturating acid conditions,[17] Figure 2A. Under nonsaturating conditions of acid, the catalytic current (i_{cat}) is linearly dependent on acid concentration indicating the current is limited by acid diffusion to the electrode surface.[25] Plots of i_{cat}/i_p vs $[H^+]$, where i_p is the cathodic peak current in the absence of acid, at multiple scan rates, Figure 2B, confirm the second-order dependence on acid concentration.[28]

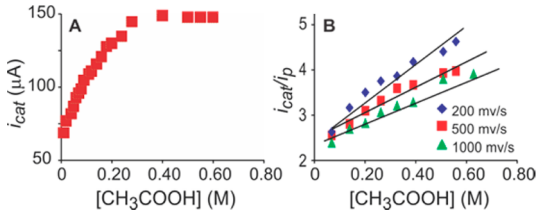

Figure 2. (A) Plot of catalytic current (μA) versus acetic acid concentration (M) for 3 mM ReL_3 at a scan rate of 200 mV/s in CH_2Cl_2 (0.1 M Bu_4NPF_6). (B) Plot of relative catalytic current versus acetic acid concentration (mM) for 3 mM ReL_3 at a scan rates of 200, 500, and 1000 mV/s.

Additionally, varying ReL_3 concentrations at a fixed $[H^+]$ confirms a first-order dependence on the catalyst concentration, see Supporting Information. Overall, the rate law for hydrogen evolution is third-order with a rate constant $k = 184$ M^{-2} s^{-1}. The rate constant is approximately 200 times lower than the corresponding value for Dubois' Mo−S dimer metal thiolate, $k = 3.7 \times 10^4$ M^{-2} s^{-1}.[29]

Further mechanistic insights were obtained by reduction of deuterated acid substrates. Our ReL_3 catalyst exhibits a large kinetic isotope effect (KIE) of 9 ± 1 for both CH_3CO_2H/CD_3CO_2D and CF_3SO_3H/CF_3SO_3D. The similarities of the KIE values for strong and weak acids further support a common rate-determining step. The large value of the KIE suggests the rate-determining step is H_2 release with significant catalyst-hydrogen bond breaking occurring at the transition state. Despite the significant number of electrocatalysts reported for HERs, relatively few studies have reported KIE data. Gray and co-workers reported an inverse KIE with values ranging from 0.54−0.57.[30] A similar inverse value observed by Fukuzumi was attributed to rate-determining metal hydride formation via proton coupled electron transfer.[31] The relatively high KIE values for ReL_3 as compared to the inverse KIE observed for metal hydrides by Gray, indicate a clearly different mechanism for H_2 evolution. Markedly, Fukuzumi recently reported a KIE of 40 for H_2 evolution with $[Ir^{III}(Cp^*)(H_2O)(bpm)Ru^{II}(bpy)_2](SO_4)_2$ {Cp* = η^5-pentamethylcyclopentadienyl, bpm = 2,2′-bipyrimidine, bpy = 2,2′-bipyridine} attributing the unusually high KIE to large tunneling effects during catalytic H_2 evolution reactions.[32] In lieu of this, further temperature-dependent studies are underway to assess the possibility of tunneling with ReL_3.

Based on the second-order acid dependence in the rate law and the large KIE, we assign the rate-determining step of our HER to H_2 release from the H_2 evolving intermediate $[ReL_3{\cdot}H_2]$, Scheme 2 (top). The cyclic voltammetry studies clearly demonstrate that both electrons must be delivered prior to the H_2 evolution step. We can discount a catalytic route involving a single reduction prior to H_2 release (via $[ReL_3{\cdot}H_2]^+$) since this route proceeds through the monothiol complex $[Re(LH)L_2]^+$, which is reduced at potentials significantly more positive than the catalytic event. As shown in Figure 1A, under catalytic conditions the cyclic voltammogram contains redox events associated with $[ReL_3]^n$ and $[Re(LH)L_2]^n$, in addition to the catalytic event. Potentials associated with $[Re(LH)L_2]^{2+/+}$ and $[Re(LH)L_2]^{+/0}$ are observed at 0.18 and −0.84 V, respectively. These values are shifted by +0.52 and +0.76 V relative to $[ReL_3]^{+/0}$ and $[ReL_3]^{0/-}$, respectively, consistent with protonation of a single thiolate donor.[33,34]

Whereas reduction of $[ReL_3{\cdot}H_2]^+$ is the final step of hydrogen evolution, hydrogen oxidation proceeds through sequential

DOI: 10.1021/jacs.5b05561
J. Am. Chem. Soc. 2015, 137, 9238−9241

Scheme 2. Electrocatalytic H_2 Evolution/Oxidation Cycles

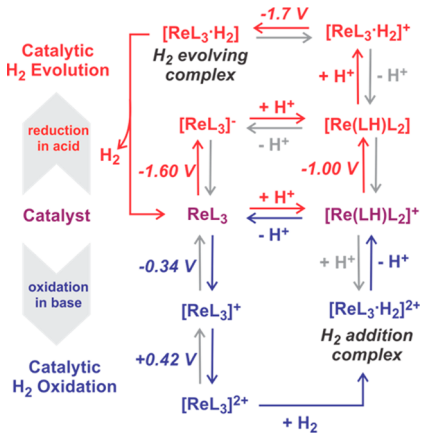

oxidations followed by H_2 addition. Oxidation of ReL_3 by two electrons in the presence of H_2 generates the hydrogen addition complex, $[ReL_3{\cdot}H_2]^{2+}$. Stepwise deprotonation with two equivalents of triethylamine regenerates ReL_3 via $[Re(LH)L_2]^+$, Scheme 2 (bottom).

The thiolate complexes $[ReL_3]^n$ in Scheme 2 are known including the structural determination of ReL_3.[35] The monoprotonated complex $[Re(LH)L_2]^+$, which acts as an intermediate in both the H_2 evolution and H_2 oxidation cycles, has been unequivocally determined via X-ray crystallography, Figure 3.[36]

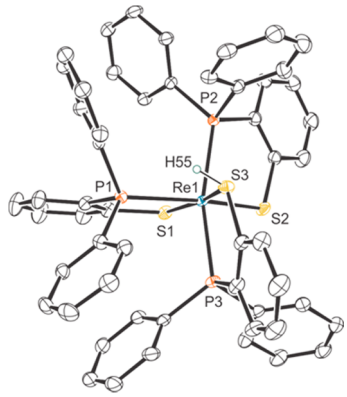

Figure 3. ORTEP representation of $[Re(LH)L_2]^+$. Full crystallographic details available in Supporting Information.

Its reduced derivative $[Re(LH)L_2]$ has been observed as a pink species in solution but has not yet been isolated. High quality single crystals of $[Re(LH)L_2]PF_6$, obtained as a degradation product of $[ReL_3{\cdot}C_2H_4]PF_6$ in methanol, reveal S3 as thiol through the location and subsequent refinement of the proton H55. The S3−H55 bond distance is 1.077(18) Å with a Re1−S3−H55 bond angle of 105.8(18)°. The structure was confirmed by X-ray analysis of $[Re(LH)L_2]^+$ as the triflate salt prepared upon protonation of ReL_3 with triflic acid, see Supporting Information. A comparison of metric parameters for ReL_3, $[Re(LH)L_2]^+$, and $[ReL_3{\cdot}C_2H_4]^{2+}$ is provided in the Supporting Information.[18,35] Addition of strong acids to solutions of $[Re(LH)L_2]^+$ results in a color change from purple to yellow-brown, although we have not yet been able to isolate $[ReL_3{\cdot}H_2]^{2+}$or its reduced derivatives.

At this time, the electronic structures of the hydrogen evolving complex $[ReL_3{\cdot}H_2]$ and the hydrogen addition complex $[ReL_3{\cdot}H_2]^{2+}$ remain unresolved. The hydrogen evolving complex $[ReL_3{\cdot}H_2]$ may contain a Re(I)-dithiol $[Re^I(LH)_2L]$ or a Re(III)-hydride $[HRe^{III}(LH)L_2]$ depending on whether the addition of the second proton occurs at the ligand or metal center. While Re(III)-hydrides have been reported in the literature,[37,38] we tentatively favor the Re(I)-dithiol representation as our complex is sterically crowded, kinetically inert, and coordinatively saturated with documented ligand-centered reactivity consistent with redox noninnocence. Likewise, our tentative assignment of the hydrogen addition complex $[ReL_3{\cdot}H_2]^{2+}$ is a Re(III)-dithiol $[Re^{III}(LH)_2L]^{2+}$, although a Re(V)-hydride description cannot be completely excluded at this time.

Despite the uncertainty regarding the nature of $[ReL_3{\cdot}H_2]$ and $[ReL_3{\cdot}H_2]^{2+}$, the isoelectronic dithioether derivatives $[ReL_3{\cdot}C_2H_4]$ and $[ReL_3{\cdot}\ C_2H_4]^{2+}$ have been studied in more detail.[18,19,39] As we previously reported, $[ReL_3{\cdot}C_2H_4]^{2+}$ is a structurally characterized dithioether complex formed upon the two electron oxidation of ReL_3 in the presence of ethylene. Notably, while $[ReL_3{\cdot}C_2H_4]^{2+}$ strongly binds ethylene ($K = 2.5 \times 10^9\ M^{-1}$), reduction by one electron to $[ReL_3{\cdot}C_2H_4]^+$ dramatically reduces the binding affinity ($K = 4.0\ M^{-1}$) resulting in dynamic, reversible ethylene binding.[19] Further reduction to the neutral complex $[ReL_3{\cdot}C_2H_4]$ results in full release of ethylene ($K = 1.9 \times 10^{-11}\ M^{-1}$). The latter complex is isoelectronic with the hydrogen evolving complex $[ReL_3{\cdot}H_2]$.

Similar to the low ethylene binding affinity of the neutral $[ReL_3{\cdot}C_2H_4]$,[18,19] the H_2 evolving complex $[ReL_3{\cdot}H_2]$ would be expected to have a relatively low H_2 binding affinity based on the $[ReL_3{\cdot}H_2]^{+/0}$ reduction potential (see Supporting Information). Release of ethylene from $[ReL_3{\cdot}C_2H_4]$ occurs via heterolytic (Scheme 3) or homolytic (not shown) C−S bond cleavage with a

Scheme 3. Analogy between Ethylene Release from $[ReL_3{\cdot}C_2H_4]$ and Hydrogen Release from $[ReL_3{\cdot}H_2]$

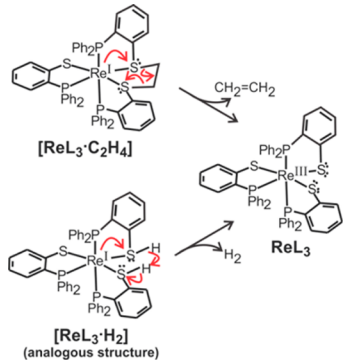

net 2-electron oxidation of the metal complex and a 2-electron reduction of the ligand.[18,19] A similar route could be envisaged for $[ReL_3{\cdot}H_2]$ assuming a Re(I)-dithiol $[Re^I(LH)_2L]$ electronic structure, Scheme 3. Likewise, ligand-centered H_2 addition to $[ReL_3{\cdot}H_2]^{2+}$ would generate $[ReL_3{\cdot}H_2]^{2+}$ as the Re(III)-dithiol $[Re^{III}(LH)_2L]^{2+}$, analogous to formation of the stable $[ReL_3{\cdot}C_2H_4]^{2+}$ complex.[18]

In summary, ReL_3 catalytically evolves H_2 upon reduction under acidic conditions and catalytically oxidizes H_2 upon oxidation under basic conditions. While the exact nature of the H_2 evolving complex $[ReL_3{\cdot}H_2]$ and the H_2 addition complex $[ReL_3{\cdot}H_2]^{2+}$ remain unresolved, the species are isoelectronic with derivatives prepared from the redox-regulated addition of ethylene to ReL_3, suggesting ligand-centered reactivity. While unprecedented in homogeneous mononuclear systems, Xu et al.

DOI: 10.1021/jacs.5b05561
J. Am. Chem. Soc. 2015, 137, 9238−9241

recently reported heterogeneous H_2 evolution from MoS_2 proposing exposed unsaturated S edge atoms as reaction sites.[40] The unique reactivity of ReL_3 could be attributed to a sterically crowded, kinetically inert, and coordinatively saturated metal center that prevents facile formation of metal hydride, which is proposed for other active metal−sulfur catalysts. While this would normally be expected to render a complex inactive, the noninnocent ligands in ReL_3 are known to react with small molecule substrates, which opens the possibility of a ligand-centered pathway. This could explain the unusual KIE and bifunctional (H_2 evolution and H_2 oxidation) activity of ReL_3, although further experimental and computational investigations are necessary to confirm if catalysis with ReL_3 is indeed ligand-centered.

■ ASSOCIATED CONTENT

Supporting Information

Experimental methods, experimental data, and sample calculations in PDF format and crystallographic data in CIF format (CCDC 1403507 and 1410091). The Supporting Information is available free of charge on the ACS Publications website at DOI: 10.1021/jacs.5b05561.

■ AUTHOR INFORMATION

Corresponding Author

*grapperhaus@louisville.edu

Notes

The authors declare no competing financial interest.

■ ACKNOWLEDGMENTS

Acknowledgment is made to the National Science Foundation (CHE-1361728) for funding. M.S.M. thanks the Department of Energy (DE-FG02-08CH11538) and the Kentucky Research Challenge Trust Fund for the upgrade of our X-ray facilities.

■ REFERENCES

(1) Lewis, N. S.; Nocera, D. G. *Proc. Natl. Acad. Sci. U. S. A.* **2006**, *103*, 15729−15735.

(2) Barton, B. E.; Olsen, M. T.; Rauchfuss, T. B. *Curr. Opin. Biotechnol.* **2010**, *21*, 292−297.

(3) Darensbourg, M. Y.; Lyon, E. J.; Zhao, X.; Georgakaki, I. P. *Proc. Natl. Acad. Sci. U. S. A.* **2003**, *100*, 3683−3688.

(4) Fontecilla-Camps, J. C.; Volbeda, A.; Cavazza, C.; Nicolet, Y. *Chem. Rev.* **2007**, *107*, 4273−4303.

(5) Shima, S.; Pilak, O.; Vogt, S.; Schick, M.; Stagni, M. S.; Meyer-Klaucke, W.; Warkentin, E.; Thauer, R. K.; Ermler, U. *Science* **2008**, *321*, 572−575.

(6) Jacobsen, G. M.; Yang, J. Y.; Twamley, B.; Wilson, A. D.; Bullock, R. M.; DuBois, M. R.; DuBois, D. L. *Energy Environ. Sci.* **2008**, *1*, 167−174.

(7) Rakowski Dubois, M.; Dubois, D. L. *Acc. Chem. Res.* **2009**, *42*, 1974−1982.

(8) Wiedner, E. S.; Yang, J. Y.; Dougherty, W. G.; Kassel, W. S.; Bullock, R. M.; DuBois, M. R.; DuBois, D. L. *Organometallics* **2010**, *29*, 5390−5401.

(9) Wiese, S.; Kilgore, U. J.; DuBois, D. L.; Bullock, R. M. *ACS Catal.* **2012**, *2*, 720−727.

(10) Gan, L.; Groy, T. L.; Tarakeshwar, P.; Mazinani, S. K. S.; Shearer, J.; Mujica, V.; Jones, A. K. *J. Am. Chem. Soc.* **2015**, *137*, 1109−1115.

(11) Karunadasa, H. I.; Chang, C. J.; Long, J. R. *Nature* **2010**, *464*, 1329−1333.

(12) McNamara, W. R.; Han, Z. J.; Alperin, P. J.; Brennessel, W. W.; Holland, P. L.; Eisenberg, R. *J. Am. Chem. Soc.* **2011**, *133*, 15368−15371.

(13) McNamara, W. R.; Han, Z. J.; Yin, C. J.; Brennessel, W. W.; Holland, P. L.; Eisenberg, R. *Proc. Natl. Acad. Sci. U. S. A.* **2012**, *109*, 15594−15599.

(14) Singh, W. M.; Baine, T.; Kudo, S.; Tian, S. L.; Ma, X. A. N.; Zhou, H. Y.; DeYonker, N. J.; Pham, T. C.; Bollinger, J. C.; Baker, D. L.; Yan, B.; Webster, C. E.; Zhao, X. *Angew. Chem., Int. Ed.* **2012**, *51*, 5941−5944.

(15) Zarkadoulas, A.; Koutsouri, E.; Mitsopoulou, C. A. *Coord. Chem. Rev.* **2012**, *256*, 2424−2434.

(16) Weber, K.; Krämer, T.; Shafaat, H. S.; Weyhermüller, T.; Bill, E.; van Gastel, M.; Neese, F.; Lubitz, W. *J. Am. Chem. Soc.* **2012**, *134*, 20745−20755.

(17) Wilson, A. D.; Newell, R. H.; McNevin, M. J.; Muckerman, J. T.; DuBois, M. R.; DuBois, D. L. *J. Am. Chem. Soc.* **2006**, *128*, 358−366.

(18) Grapperhaus, C. A.; Ouch, K.; Mashuta, M. S. *J. Am. Chem. Soc.* **2009**, *131*, 64−65.

(19) Ouch, K.; Mashuta, M. S.; Grapperhaus, C. A. *Inorg. Chem.* **2011**, *50*, 9904−9914.

(20) Grapperhaus, C. A.; Kozlowski, P. M.; Kumar, D.; Frye, H. N.; Venna, K. B.; Poturovic, S. *Angew. Chem., Int. Ed.* **2007**, *46*, 4085−4088.

(21) Grapperhaus, C. A.; Poturovic, S. *Inorg. Chem.* **2004**, *43*, 3292−3298.

(22) Andrieux, C. P.; Blocman, C.; Dumasbouchiat, J. M.; Mhalla, F.; Saveant, J. M. *J. Electroanal. Chem. Interfacial Electrochem.* **1980**, *113*, 19−40.

(23) Felton, G. A. N.; Vannucci, A. K.; Chen, J. Z.; Lockett, L. T.; Okumura, N.; Petro, B. J.; Zakai, U. I.; Evans, D. H.; Glass, R. S.; Lichtenberger, D. L. *J. Am. Chem. Soc.* **2007**, *129*, 12521−12530.

(24) Fourmond, V.; Jacques, P. A.; Fontecave, M.; Artero, V. *Inorg. Chem.* **2010**, *49*, 10338−10347.

(25) Saveant, J. M.; Su, K. B. *J. Electroanal. Chem. Interfacial Electrochem.* **1984**, *171*, 341−349.

(26) Darmon, J. M.; Raugei, S.; Liu, T.; Hulley, E. B.; Weiss, C. J.; Bullock, R. M.; Helm, M. L. *ACS Catal.* **2014**, *4*, 1246−1260.

(27) Roberts, J. A. S.; Bullock, R. M. *Inorg. Chem.* **2013**, *52*, 3823−3835.

(28) Hu, X. L.; Brunschwig, B. S.; Peters, J. C. *J. Am. Chem. Soc.* **2007**, *129*, 8988−8998.

(29) Appel, A. M.; DuBois, D. L.; DuBois, M. R. *J. Am. Chem. Soc.* **2005**, *127*, 12717−12726.

(30) Marinescu, S. C.; Winkler, J. R.; Gray, H. B. *Proc. Natl. Acad. Sci. U. S. A.* **2012**, *109*, 15127−15131.

(31) Kotani, H.; Hanazaki, R.; Ohkubo, K.; Yamada, Y.; Fukuzumi, S. *Chem. - Eur. J.* **2011**, *17*, 2777−2785.

(32) Fukuzumi, S.; Kobayashi, T.; Suenobu, T. *J. Am. Chem. Soc.* **2010**, *132*, 1496−1497.

(33) Sellmann, D.; Mahr, G.; Knoch, F.; Moll, M. *Inorg. Chim. Acta* **1994**, *224*, 45−59.

(34) Zhong, F.; Lisi, G. P.; Collins, D. P.; Dawson, J. H.; Pletneva, E. V. *Proc. Natl. Acad. Sci. U. S. A.* **2014**, *111*, E306−315.

(35) Dilworth, J. R.; Hutson, A. J.; Morton, S.; Harman, M.; Hursthouse, M. B.; Zubieta, J.; Archer, C. M.; Kelly, J. D. *Polyhedron* **1992**, *11*, 2151−2155.

(36) Crystal data for $[Re(LH)L_2]PF_6$: purple prism, monoclinic, space group $P2_1/c$, a = 9.59553(9) Å, b = 33.0018(3) Å, c = 15.41951(15) Å, α = 90°, β = 97.5416(10)°, γ = 90°, V = 4840.66(8) Å^3, r_{calcd} = 1.663 Mg/m^3, Z = 4. Data were collected on an Agilent Technologies Gemini CCD diffractometer using Mo Ka radiation. For all 13,986 unique reflections [R(int) = 0.0281], the final anisotropic full-matrix least-squares refinement on F^2 for 598 variables converged at R_1 = 0.033, wR_2 = 0.078 with a GOF of 1.09. CCDC 1403507 and 1410091 contain supplementary crystallographic data.

(37) Hoffman, D. M.; Lappas, D.; Putilina, E. *Inorg. Chem.* **1992**, *31*, 79−81.

(38) Gusev, D. G.; Nietlispach, D.; Eremenko, I. L.; Berke, H. *Inorg. Chem.* **1993**, *32*, 3628−3636.

(39) Lu, M.; Campbell, J. L.; Chauhan, R.; Grapperhaus, C. A.; Chen, H. *J. Am. Soc. Mass Spectrom.* **2013**, *24*, 502−512.

(40) Yan, Y.; Xia, B.; Xu, Z.; Wang, X. *ACS Catal.* **2014**, *4*, 1693−1705.

DOI: 10.1021/jacs.5b05561
J. Am. Chem. Soc. 2015, 137, 9238−9241